Polymer 50 (2009) 654–661

Contents lists available at ScienceDirect

Polymer

journal homepage: www.elsevier.com/locate/polymer

Modeling water states in polyvinyl alcohol-fumed silica nano-composites

Shingjiang Jessie Lue*, Song-Jiang Shieh

Department of Chemical and Materials Engineering and Green Technology Research Center, Chang Gung University, 259 Wen-Hwa First Road, Kwei-shan, Taoyuan 333, Taiwan

ARTICLE INFO

Article history:
Received 29 April 2008
Received in revised form
30 October 2008
Accepted 17 November 2008
Available online 27 November 2008

Keywords:
Water states
Bound water
Polymer–filler nano-composites

ABSTRACT

We proposed a mathematical model to account for water contents in different states as a function of filler concentration in polymer–filler composites. The water states were characterized in polyvinyl alcohol (PVA) and PVA–fumed silica (FS) composites using low temperature differential scanning calorimetry. This model takes into consideration the inert filler dilution effect, the equilibrium of bound water to free and freezable water states associated with FS nano-particles, and the suppressed hydrogen-bonding ability of hydroxyl groups in polymer chains caused by FS shielding. Predicted results were in excellent agreement with experimental data. This model can yield a great understanding of the distribution of water states into bound and free (and freezable) water states for homogeneous, heterogeneous or micro-phase separated polymers, and especially perfluorosulfonic acid membranes and water-retaining hydrogels.

1. Introduction

Various water states in polymers have been studied in the last few decades. Differential scanning calorimetry (DSC) [1–3], nuclear magnetic resonance (NMR) [4,5], infrared (IR) spectroscopy [6], Raman spectroscopy [7] and dielectric response [8] are valuable tools to determine the partitioning of water into various states. At least three states have been identified for moistened hydrophilic membranes (e.g., polyvinyl alcohol (PVA)), including: (i) free water, (ii) freezable bound or intermediate water, and (iii) unfrozen or bound water. Free water possesses the same physical characteristics as bulk water, which freezes at temperatures close to 0° C. Thus, this state is also called as freezing or freezable water. The second state freezes at a lower temperature in comparison with free water. Other terms used for this super-cooled freezable water include freezable bound water and intermediate water [7,9]. This state may originate from impure water clusters [5], water molecules confined to small pores [10], or physical interaction with the polymer backbone matrix [7,11]. The third state of water, unfrozen or bound water, has no detectable phase transition when using differential scanning calorimetry (DSC). Bound water is postulated to form hydrogen bonding between water molecules and polar polymer groups. However, other mechanisms may also play an important role in this phenomenon. Liu and Yao [9] suggested that isolated water molecules entrapped in nanometer-size cavities can develop this state of water. Lue and Yang [12] showed that organic solvents can also form non-freezable states in polydimethylsiloxane membranes, as a result of hydrophobic interactions between penetrating molecules and polymer chains.

Water states have importance in many fields. For example, unfrozen bound water contributes to the stability of proteins [13], enzyme activity [14], drug delivery behavior [15], and pharmaceutical devices [16,17]. Previous researches have also shown that dense membranes with high bound water content can enhance water permeability in reverse osmosis and pervaporation processes, owing to the plasticizing effect of bound water [1,18,19]. For fuel cell applications, water states in solid electrolytes have recently gained much attention. It has been demonstrated that practical proton conductivities can only be achieved when there is a sufficient amount of bound and free water in the solid electrolytes [7,18].

The objective of this study is to investigate water states in heterogeneous composites. PVA hybrid membranes containing various amounts of nano-sized fumed silica (FS) were used as the model matrix. Free and bound water contents as a function of total water uptake and FS fraction were determined. A mathematical model has been proposed to elucidate interactions between water and PVA, as well as between water and FS.

2. Experimental

2.1. Membrane preparation

Polyvinyl alcohol (89 000–98 000 MW; >99% degree of hydrolysis) was obtained from Sigma–Aldrich (St. Louis, MO, USA). PVA crystallinity, as determined with DSC, was found to be 51.45% [20]. FS was purchased from Cabot Corp. (Carbosil® M5, Tuscola, IL, USA).

* Corresponding author. Tel.: +886 3 2118800x5489; fax: +886 3 2118700.
E-mail address: jessie@mail.cgu.edu.tw (S.J. Lue).

0032-3861/$ – see front matter © 2008 Elsevier Ltd. All rights reserved.
doi:10.1016/j.polymer.2008.11.026

Nomenclature

c_p	Specific heat capacity (J/gK)
ΔH	Water fusion enthalpy (J/g water or J/g swollen membrane)
K	Equilibrium constant between bound and free (including freezable) water associated with filler
M	Mass of membrane (g)
T	Temperature (K)
W	Water content (g/g membrane)
W'	Water content in composite when FS acts as a diluter (g/g composite)
W''	Water content in composite when FS acts as both a diluter and hydrogen-bonding suppresser (g/g composite)

Subscript

b	Bound water
c	Critical
d	Dried film
f	Free or freezable water
m	Moistened film
PVA	Pure PVA film
t	Total
w	Water

Greek letters

ϕ	Filler mass fraction
γ	Number of water molecules per SiO_2 molecule (mol/mol)
λ	Number of water molecules per hydroxyl group in PVA (mol/mol)
ξ	Hydrogen-bonding hindrance coefficient due to FS

PVA was dissolved in pure water to form a 15% (wet basis) polymer solution. A predetermined amount of FS was then added to this solution. The mixture was heated at 90 °C, with agitation, for 6 h and subsequently degassed in an ultrasonic bath. Resulting slurry was cast on a glass plate using an applicator knife (AP-M04, Gardner Co., Inc., Pompano Beach, FL, USA). Water in the film was allowed to evaporate at room temperature for 1 day. Afterward, the film was dried in a vacuum oven at 60 °C for 8 h. Using a coating thickness gauge (model 345, Elcometer Instrument Ltd., Edge Lane, UK), the final composite membrane thickness was measured at 100 ± 10 μm.

2.2. DSC measurement

Pure water (from a Millipore water purifier, Elix5/Milli-Q Gradient system, Millipore Corp., Bedford, MA, USA) was sealed in a pre-weighed DSC aluminum pan. A final mass (water sample plus DSC pan) was taken and the mass difference between this and the empty DSC pan was recorded. The sealed pan was placed in a DSC analyzer (DSC Q10, TA Instruments, New Castle, DE, USA), cooled to −40 °C at a rate of 20 °C/min, then heated to 40 °C at a rate of 5 °C/min. The enthalpy of the pure water at 0 °C (ΔH_w^o) was used to calculate free and freezable water contents in PVA composites.

Dried fumed silica was suspended underneath a microbalance (model BP211D, Sartorius AG, Goettingen, Germany) and immersed in a saturated water vapor at 25 °C. After three and four days, the moistened fumed silica was sealed in a DSC pan and the water fusion enthalpy was determined.

PVA and PVA–FS composites were dried until a constant weight was achieved. Approximately 250 mg of dry film was measured (M_d) and immersed in pure water at 25 °C. The film was removed from water at different elapsed times and blotted with tissue paper to eliminate any liquid water adhered to the surface. Weight of the moistened sample (M_m) was measured and the total water content (W_t) was calculated according to the equation:

$$W_t = (M_m - M_d)/M_d \quad (1)$$

where W_t is the water uptake mass per gram of dry composite membrane (g/g-dry membrane), M is the mass, and the subscripts m and d represent moisten and dry membranes, respectively.

Afterward, a portion of the wet sample was cut (5–15 mg) and sealed in a pre-weighed DSC aluminum pan. The water enthalpies in the PVA and PVA–FS composites were measured as aforementioned. To calculate the free and freezable water content (W_f), a summation of the endothermic enthalpies (ΔH) at peak temperatures of −12 to 0 °C was performed.

$$W_f = \Delta H(1 + W_t)/\Delta H_w \quad (2)$$

where W_f is the free and freezable water content (g/g membrane, dry basis), ΔH is the sum of enthalpies from the DSC thermogram (J/g swollen membrane). A factor of $(1 + W_t)$ was used to convert enthalpy (ΔH) with units of J/g swollen membrane into its corresponding value with units of J/g-dry membrane. The value of ΔH_w is the melting enthalpy of pure water at the corresponding fusion temperature and can be estimated using the following equation.

$$\Delta H_w = \Delta H_w^o - \Delta c_p \Delta T \quad (3)$$

where ΔH_w^o is the pure water enthalpy at 0 °C, Δc_p is the specific heat capacity between the liquid water and solid ice, ΔT is the freezing point depression.

Non-freezable bound water content (W_b) was estimated by subtracting the free and freezable bound water content from the total water content.

$$W_b = W_t - W_f \quad (4)$$

3. Results

3.1. DSC thermograms

DSC thermograms for pure water and dry PVA film are shown in Fig. 1. The PVA did not reveal any phase transition within the scanned temperature range. The endothermic peak of water results from the enthalpy change during bulk water melting at about 0 °C (334.5 J/g). This value, after corrected for fusion temperature depression (as shown in Eq. (3) [2]), was used to calculate the free and freezable bound water content, as shown in Eq. (2). This pure water enthalpy value was not significantly different from the previously reported water fusion enthalpies (333–334 J/g [12,21]). The value determined here was used for subsequent calculations in this report.

The fumed silica, saturated with water vapor for three and four days, absorbed 0.024 g/g and 0.047 g/g water vapor, respectively. The moistened fumed silica was sealed in a DSC pan and the water fusion enthalpy was determined. The sample with 0.024 g/g vapor content did not reveal any water fusion enthalpy (Fig. 2). The sample with higher water content (0.047 g/g) showed a broad fusion enthalpy peak at −10 °C (Fig. 2), indicating the presence of both freezable and bound water. The water contents for freezable and bound waster were about 0.01 g/g and 0.03 g/g, respectively. However, these numbers were subject to large experimental error due to the small enthalpy which was at the range of the detection limit of the instrument. There was no water loss before and after the DSC measurement.

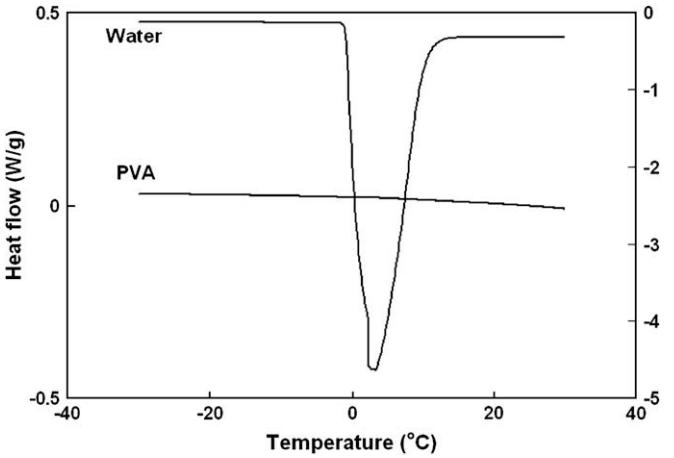

Fig. 1. DSC thermograms of pure water (right axis) and dry PVA (left axis).

Thermograms for moistened PVA and PVA–FS membranes at various total water uptakes are shown in Figs. 3 through 6. At low sorption levels, no water fusion peak was present in the scanned temperature range (e.g., a and b in Figs. 3 through 6). For intermediate sorption levels (between 0.7 and 1.5 g/g-membrane) two fusion peaks were discovered. The fusion peak at ~0 °C is from ice crystal melting upon heating. Therefore, this quantity is referred to as free water [1]. This free water exhibits a fairy constant melting temperature for both PVA and PVA–FS composites. Another broad endothermic peak was detected at a lower temperature, ranging, from −12 to −4 °C. Presence of this freezable water indicates the occurrence of disordered, incomplete ice crystals [5] or liquid-like water confined in dynamic pores [10]. An alternative name for this water state is "freezable bound water" [2]. The melting point depression of freezable bound water diminished with water content for both PVA and PVA–FS composites. At higher water content, the melting peak of freezable water tends to shift toward that of free water. These two became indistinguishable above 1.5 g/g-membrane water content (e.g., f and g in Figs. 3 and 4).

3.2. Water fusion enthalpy

Many studies have summarized the free and freezable bound contents as one measure [2,22,23]. Combined endothermic enthalpies (ΔH) for free and freezable water as a function of water uptake in PVA and PVA–FS composites are demonstrated in Fig. 7. For all membranes there was no fusion enthalpy below a critical value. A regression line for PVA film is shown as a solid curve in

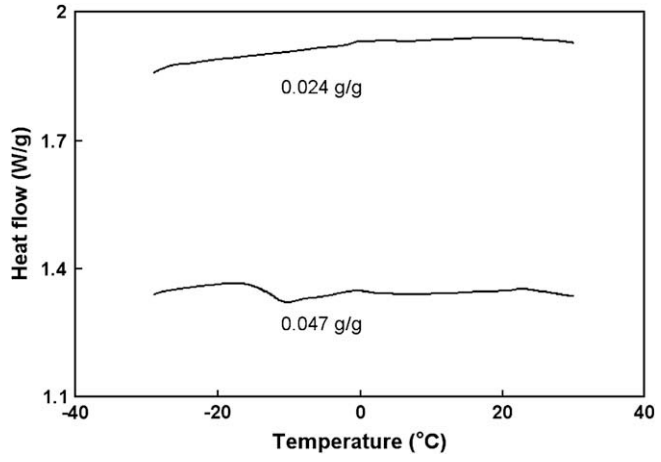

Fig. 2. DSC thermograms of fumed silica containing 0.024 g/g and 0.047 g/g water.

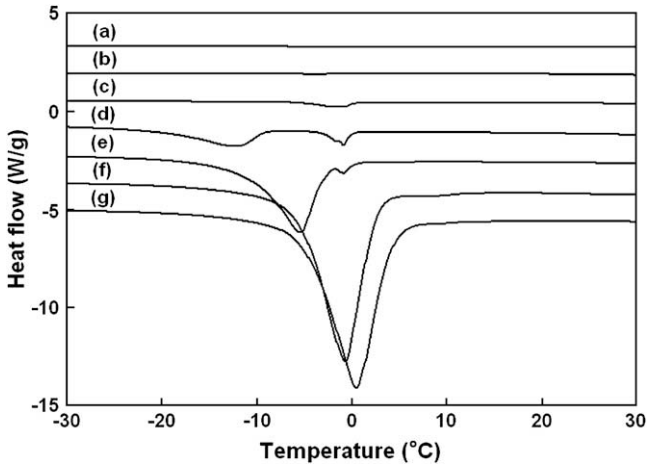

Fig. 3. DSC thermograms of moistened PVA membranes at various water contents. (a) 0.151; (b) 0.421; (c) 0.692; (d) 0.850; (e) 1.300; (f) 2.236; (g) 2.426 g/g-membrane.

Fig. 7. From this regression analysis, the critical value was determined to be 0.675 ± 0.066 (mean ± 95% confidence interval) g/g-membrane for PVA. Below this critical value, sorbed water in PVA exhibited no water fusion properties and is considered to be in a non-freezable bound water state.

Above the 0.675 g/g critical water content, all additional sorbed water in PVA was in a freezable state and the amount of non-freezable water remained unchanged. Therefore, the increase in water fusion enthalpy per unit gram of additional sorbed water was the same as that of the pure water (i.e., freezable water). The slope of data points above 0.675 g/g water content in Fig. 7 was estimated to be 339.95 ± 20.46 J/g, which is not significantly different from the water fusion enthalpy [5,12]. Results here confirm that, above the 0.675 g/g critical water content level, additional water behaves like pure bulk water.

3.3. Free and bound water contents

Eqs. (2) and (4) were used to calculate different water states. Fig. 8 represents the water in PVA that has partitioned into bound (W_b) as well as free or freezable (W_f) water contents. Below the critical value of 0.675 g/g-membrane, all sorbed water was in the non-freezable bound state. Above the critical value, excess water exists in a free or freezable bound state. Non-freezable water

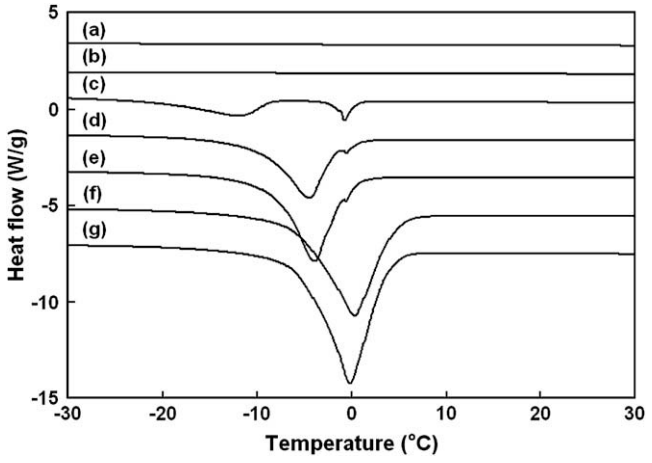

Fig. 4. DSC thermograms of moistened PVA–FS (10%) composites at various water contents. (a) 0.192; (b) 0.308; (c) 0.764; (d) 1.152; (e) 1.297; (f) 1.663; (g) 1.903 g/g-membrane.

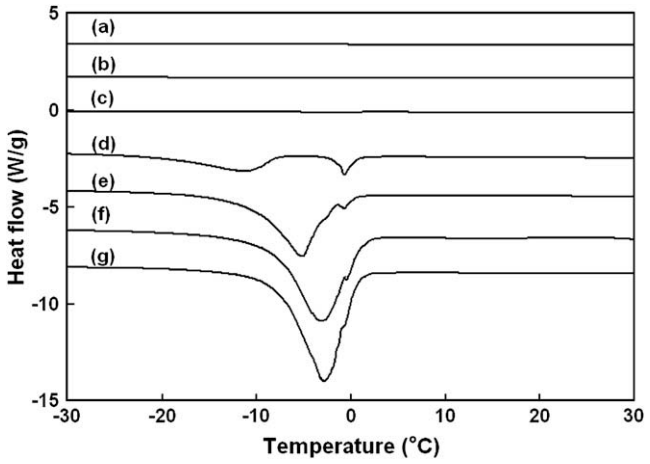

Fig. 5. DSC thermograms of moistened PVA–FS (20%) composites at various water contents. (a) 0.104; (b) 0.126; (c) 0.374; (d) 0.706; (e) 1.198; (f) 1.472; (g) 1.545 g/g-membrane.

content remained stable. Statistical analysis indicated that, in this high sorption region, non-freezable bound water content was not related to water uptake and the slope (right portion of the solid line in Fig. 8) was not significantly different from zero (with a p-value greater than 0.52 using statistical analysis).

Water states in PVA–FS composites are shown in Figs. 9 through 11. One common finding from these data is that all sorbed water was in a non-freezable bound state below a critical value. The critical water content was the highest for PVA (0.675 g/g), and decreased to 0.352 g/g with 30% FS addition into the PVA films. The decrease in the critical water content can be ascribed to a lower binding capacity due to dilution effect of FS and suppressed hydrogen binding ability from the FS particles. A detailed discussion on this value will be given in Sections 4.2, 4.3, and 4.5. Above the critical value, free and freezable water appeared; however, non-freezable bound water content showed a different trend. Contrary to the constant value found for PVA, non-freezable bound water content in PVA–FS increased with water uptake, especially for a PVA-30% FS composite. In addition, the equilibrium water content (maximum water uptake) was highest for PVA, at approximately 2.426 g/g-membrane. Equilibrium water content decreased to 1.904, 1.545, and 0.991 g/g-membrane for composites containing 10%, 20%, and 30% FS, respectively.

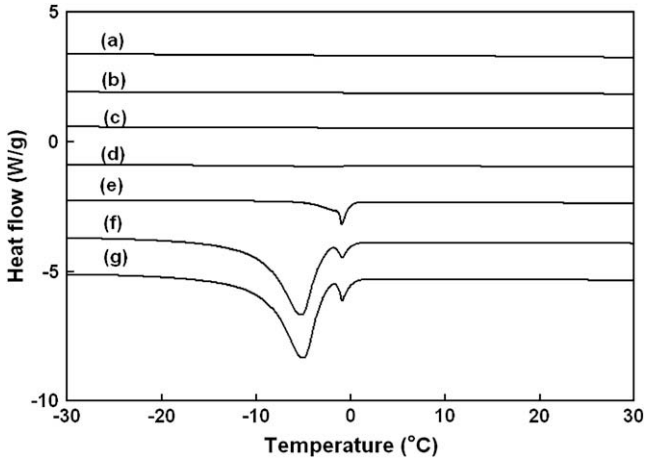

Fig. 6. DSC thermograms of moistened PVA–FS (30%) composites at various water contents. (a) 0.146; (b) 0.195; (c) 0.230; (d) 0.343; (e) 0.436; (f) 0.892; (g) 0.991 g/g-membrane.

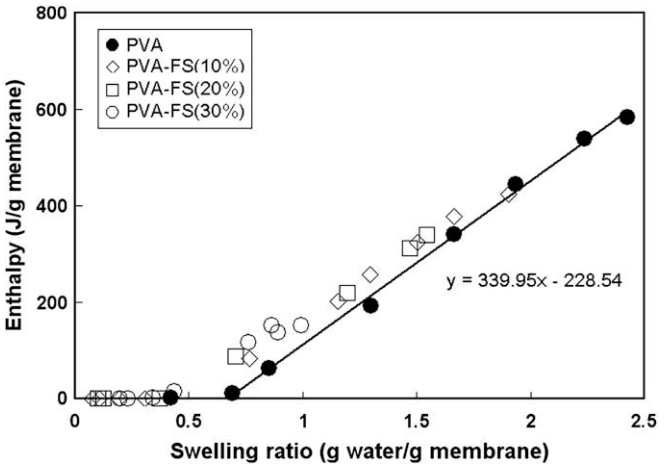

Fig. 7. Combined enthalpies of free (and freezable) bound water as a function of water uptake for various composites. The solid line represents the regression line for PVA samples.

4. Discussion

In order to determine the effect on water states of FS addition to a PVA matrix, data assessment and model development were carried out. Free water content was used to represent the combination of free and freezable bound water. With positron annihilation lifetime spectroscopy, Ito et al. found that free volume radius associated with freezable bound water molecules resembles a liquid phase in PVA containing a high concentration of water [24]. This is quite reasonable as they all represent the melting of ice crystals, the main difference lying in ice crystal perfection. In this study the combination of free and freezable bound water is referred to as freezable water. Amounts of freezable and non-freezable water were predicted for various FS proportions. This model took into consideration the inert filler dilution effect, the equilibrium of bound water to free water states associated with FS particles, and the suppressed hydrogen-bonding ability of hydroxyl groups in polymer chains caused by the FS shielding.

The number of water molecules sorbed in one PVA monomer unit (λ) can be calculated from the water content in pure PVA ($W_{t,PVA}$), and the molecular weights of water and the PVA repeating unit.

$$\lambda = W_{t,PVA} \cdot 44/18 \tag{5}$$

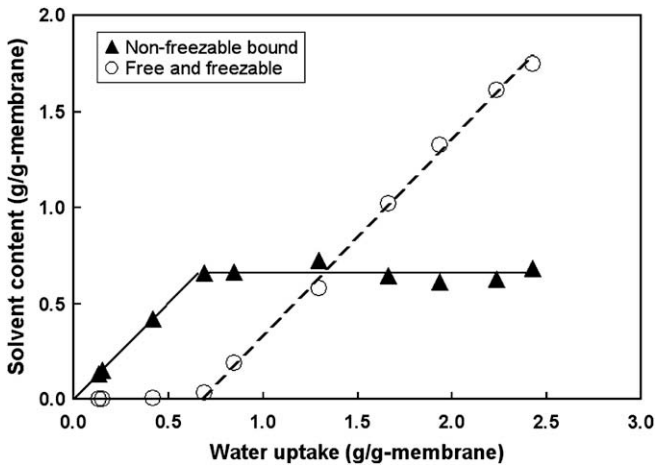

Fig. 8. Distribution of water states into non-freezable bound and free (and freezable) states for PVA in g/g-PVA unit.

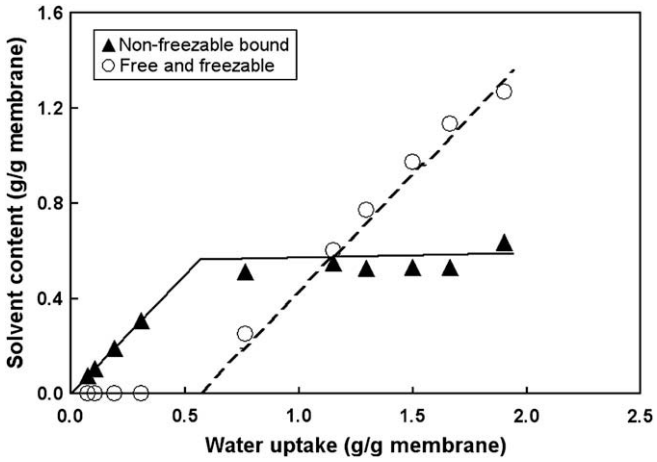

Fig. 9. Distribution of water states into non-freezable bound and free (and freezable) states for PVA–FS (10%) composite. Solid and dashed lines represent fitting results using Eq. (20).

where $W_{t,PVA}$ is the water content (g/g-PVA) in pure PVA film; 18 and 44 are the molecular weights of water and PVA repeating unit, respectively. Similarly, the number of non-freezable bound water molecules sorbed in one PVA repeating unit (λ_b) is calculated as:

$$\lambda_b = W_b \cdot 44/18 \tag{6}$$

The number of free and freezable bound water molecules sorbed in 1 mol of PVA repeating units (λ_f) is determined by subtraction:

$$\lambda_f = \lambda - \lambda_b \tag{7}$$

The distribution between λ_b and λ_f as a function of λ is expressed in Fig. 12. The critical λ value (λ_c), where free and freezable water started to appear, was extrapolated to be 1.65. PVA used in this study was 99% hydrolyzed, meaning that there were 99 hydroxyl groups for every 100 PVA repeating units. If non-freezable bound water originates from the interaction between water molecules and polymer chains, including hydrogen bonding between water molecules and hydroxyl groups in PVA polymer chains [25], then the critical value means that each PVA hydroxyl group can form 1.67 hydrogen bonds. This number is in line with the findings of Zhang et al. as well as with those of Puffr and Sebenda. Zhang et al. [2] reported 1.5 water molecules bound to each PVA unit. Puffr and Sebenda [25] found three water molecules (one tightly and two loosely bound) bound to every two amide groups in Nylon 6. On the other hand, other researchers have arrived at lower values. Nagura et al. [5] and Li et al. [22] reported that non-freezable bound content corresponded to 0.66 and 0.5 water molecules per PVA monomer unit, respectively. Gref et al. [10] discovered that one water molecule was bound to one PVA monomer in amorphous PVA. For PVA hydrogel (MW 75 K, 10% solution) with 52% crystallinity, 0.66 bound H_2O/PVA was determined [5]. The maximum number of bound water molecules which can be accommodated by each PVA unit appears to depend on many factors, including polymer crystallinity, molecular weight, polymer free volume, and chemical surroundings in the polymer matrix.

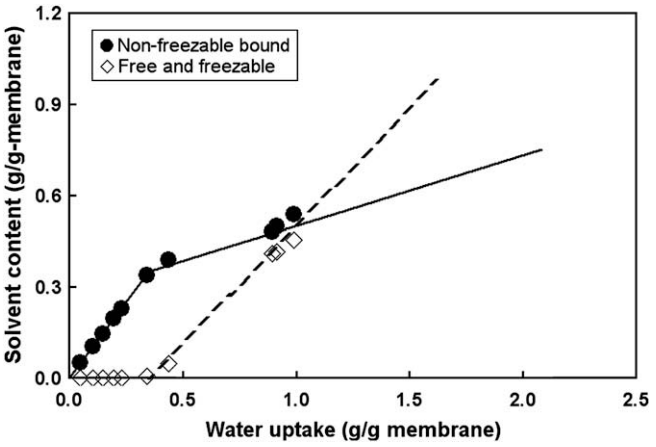

Fig. 11. Distribution of water states into non-freezable bound and free (and freezable) states for PVA–FS (30%) composite. Solid and dashed lines represent fitting results using Eq. (20).

A mathematical expression of Fig. 12 is:

$$\begin{aligned} &\lambda_b = \lambda; \lambda_f = 0 \quad \text{for } \lambda < \lambda_c \\ &\lambda_b = \lambda_c; \lambda_f = \lambda - \lambda_c \quad \text{for } \lambda \geq \lambda_c \end{aligned} \tag{8}$$

where subscripts b, c, and f stand for bound state (non-freezing), critical value, and free or freezable bound states respectively.

4.1. Inert filler dilution effect

For PVA–FS composites, FS was first treated as inert filler with a dilution effect on overall water sorption. Therefore, for a water content of W' in 1 g of composite membrane containing ϕ grams of

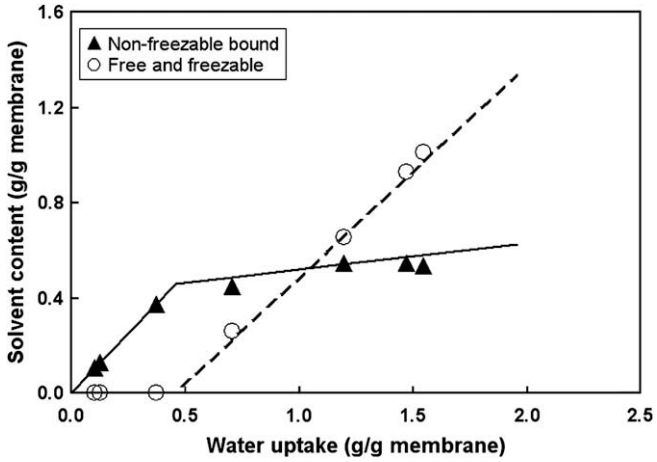

Fig. 10. Distribution of water states into non-freezable bound and free (and freezable) states for PVA–FS (20%) composite. Solid and dashed lines represent fitting results using Eq. (20).

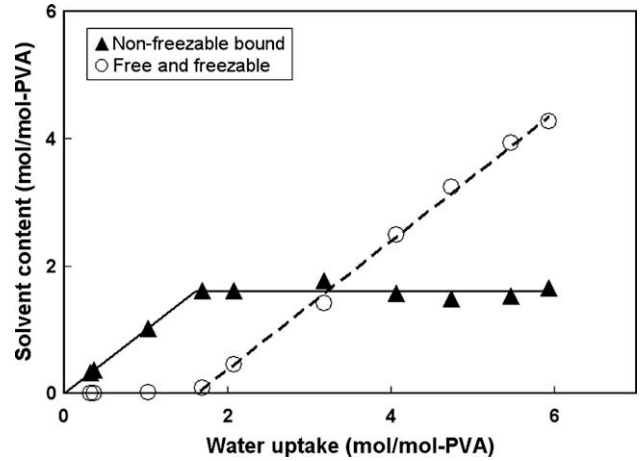

Fig. 12. Distribution of water states into non-freezable bound and free (and freezable) states for PVA in mol/mol-PVA unit. The X intercept of free (and freezable) content corresponds to the critical number of water molecules per hydroxyl group in PVA (λ_c). Solid and dashed lines represent fitting results using Eq. (8).

FS, the number of sorbed water molecules is $\lambda(1-\phi)$. Non-freezable bound and free or freezable water molecules in this system are:

$$\begin{aligned} W'_b &= 18\lambda(1-\phi)/44; W'_f = 0 \quad \text{for } \lambda < \lambda_c \\ W'_b &= 18\lambda_c(1-\phi)/44; W'_f = W' - 18\lambda_c(1-\phi)/44 \quad \text{for } \lambda \geq \lambda_c \end{aligned} \tag{9}$$

where ϕ is the FS mass fraction and W' is the mass of water molecules in 1 g of composite, when FS acts as a diluter. Eq. (9) shows the linear reduction of non-freezable bound water mass per gram of composite as FS is introduced.

4.2. Suppressed hydrogen-bonding ability of PVA

In addition to the dilution effect of FS, added FS might also form a physical cross-linker and introduce steric hindrance, keeping polymeric chains from forming hydrogen bonds or other interactions. Our recent publication shows that the nano-particles are tightly embedded in the PVA polymer matrix [26]. This shielding effect would be proportional to the ratio of filler to polymer, which equals $\phi/(1-\phi)$. Assuming application of the hindrance coefficient (ξ) to the suppressed interaction and hydrogen-bonding ability of the polymer, one would obtain Eq. (10) for the maximum non-freezing bound water content.

$$\begin{aligned} W''_b &= 18\lambda(1-\phi)(1-\xi\phi/(1-\phi))/44; W''_f = 0 \quad \text{for} \lambda < \lambda_c \\ W''_b &= 18\lambda_c(1-\phi)(1-\xi\phi/(1-\phi))/44; \\ W''_f &= W'' - 18\lambda_c(1-\phi)(1-\xi\phi/(1-\phi))/44 \quad \text{for} \lambda \geq \lambda_c \end{aligned} \tag{10}$$

where W'' is the mass of the water molecules in 1 g of composite, when FS acts as both a diluter and hydrogen-bonding suppresser. Eq. (10) shows the further reduction of critical non-freezable bound water mass per gram of composite.

4.3. Equilibrium of bound water to free water contribution from FS

Equations which were shown above are suitable to describe constant non-freezing bound water content above a critical value. To account for the gradual increase in non-freezing bound water content, as shown in Figs. 9 through 11, we propose that FS can also adsorb water consisting of free and bound states. In addition, we assume that an equilibrium is established between these two states:

$$\begin{aligned} &\text{water}_{f\text{–}FS} \leftrightharpoons \text{water}_b - \text{FS} \\ &K = [\text{water}_b - \text{FS}]/\left[\text{water}_f - \text{FS}\right] \end{aligned} \tag{11}$$

where subscripts b and f represent bound and free states, respectively, K is a fitted parameter, and water–FS stands for the interaction between water and FS. The parameter γ is defined as the number of water molecules associated with each SiO_2 unit. Therefore:

$$K = \gamma_b/\gamma_f = W_{b,FS}/W_{f,FS} \tag{12}$$

or

$$W_{b,FS} = KW_{f,FS} \tag{13}$$

where subscripts b and f represent bound and freezable water states, subscripts (b, FS) and (f, FS) are the bound and free water associated with FS.

The free (and freezable bound) water, respective to the polymer, is the same amount available to FS. In every gram of composite, there are ϕ grams of FS and $(1-\phi)$ grams of PVA. Each mole of constituent (FS and PVA) has γ_f and λ_f moles of free water, respectively. The following equation holds true as a result:

$$\lambda_f(1-\phi)/44 = \gamma_f\phi/60 \tag{14}$$

where 44 and 60 are the molecular weights of PVA repeating unit and SiO_2, respectively.

Substituting Eq. (14) into Eq. (12) yields:

$$\gamma_b = K\lambda_f(1-\phi)60/(44\phi) \tag{15}$$

Eq. (15) implies that, for low sorption levels in which all water molecules exist in a non-freezable state in PVA–FS composites, there is no free water associated with PVA ($\lambda_f = 0$). At the same time, no bound water is contributed from FS ($\gamma_b = 0$) and no free water from FS ($\gamma_f = 0$). Under this circumstance FS does not adsorb any water, as the sorbed water molecules are hydrogen-bound to PVA chains. Above the critical sorption level excess water would be in a free (and freezable) state. This water would be adsorbed by FS, with a portion of it becoming bound water with FS. Remaining water is in a free state, neither bound to FS nor to PVA.

4.4. Overall water sorption

From Eq. (10) and the discussion in the previous paragraph, one can obtain the overall bound water content at low sorption levels (below critical λ_c):

$$\begin{aligned} W_b &= 18\lambda(1-\phi)(1-\xi\phi/(1-\phi))/44 \\ W_f &= 0 \\ W_t &= W_b + W_f \quad \text{for } \lambda < \lambda_c \end{aligned} \tag{16}$$

At high sorption levels ($\lambda \geq \lambda_c$) the overall bound water content and free (or freezable) water content can be expressed as:

$$\begin{aligned} W_b &= W''_b + W_{b,FS} \\ W''_f &= W_{f,FS} \end{aligned} \tag{17}$$

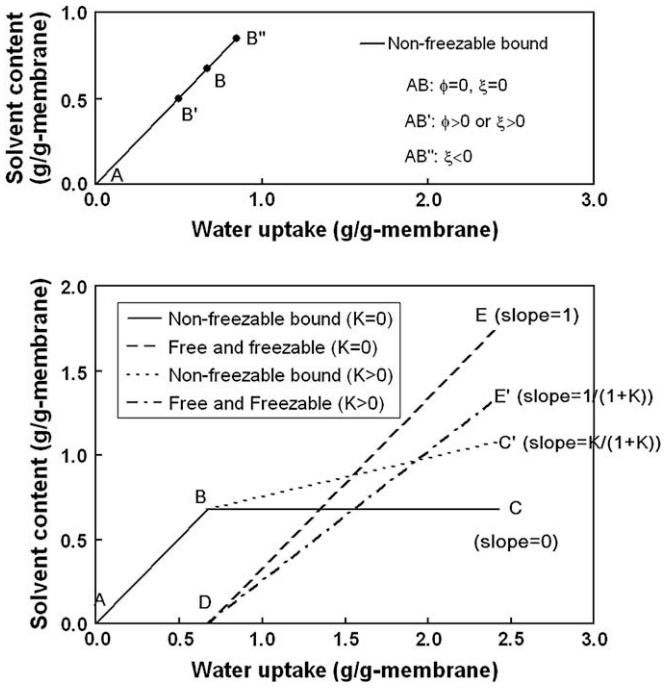

Fig. 13. Illustration of the effect of FS filler content (ϕ) and hydrogen-bonding hindrance coefficient (ξ) on maximum bound state content (upper); and the effect of the equilibrium constant (K) between bound water and free water associated with FS on water states in PVA–FS composites (lower). The values of ϕ and ξ influence the maximum bound state content (points B, B′, or B″), while the K value changes the slopes of BC and DE to BC′ and DE′ for bound water and freezable water contents, respectively.

where W is the mass of water molecules in 1 g of composite, when FS is acting as both a diluter and hydrogen-bonding suppresser and when the free and bound water associated with FS have come to equilibrium. In addition, from Eqs. (13) and (17), and including mass balance over water states, the following equation is achieved.

$$W_{b,FS} = KW_{f,FS} = KW_f'' = K(W_t - W_b'' - W_{b,FS}) \quad (18)$$

Rearranging Eq. (18) and combining it with Eq. (10) give the result:

$$\begin{aligned} W_{b,FS} &= K/(1+K)\cdot(W_t - W_b'') \\ &= K/(1+K)[W_t - 18\lambda_c(1-\phi)(1-\xi\phi/(1-\phi))/44] \end{aligned} \quad (19)$$

Combining Eqs. (10), (16), and (19), the overall bound water content and free (and freezable) water content at high sorption levels are obtained:

$$\begin{aligned} W_b &= 18\lambda_c(1-\phi)(1-\xi\phi/(1-\phi))/44 + K/(1+K)\cdot[W_t - 18\lambda_c(1-\phi)(1-\xi\phi/(1-\phi))/44] \\ W_f &= 1/(1+K)\cdot[W_t - 18\lambda_c(1-\phi)(1-\xi\phi/(1-\phi))/44] \quad \text{for} \lambda \geq \lambda_c \end{aligned} \quad (20)$$

4.5. Model adequacy and implications

Unknown parameters ξ and K, shown in Eq. (20), were fitted using data in Figs. 9 through 11. The ξ value was found to be 0.6, while K varied with FS content. The K value was 0.08 for PVA–FS (10%), 0.13 for PVA–FS (20%), and 0.42 for PVA–FS (30%). A higher percentage of FS in the composite correlated with an increase in the ratio of bound water to free water associated with FS, resulting in a higher partition coefficient (K). Predicted W_b and W_f values were plotted as solid and dashed lines, respectively, in Figs. 9 through 11. Modeled results were in excellent agreement with the experimental data, confirming the adequacy of the proposed model.

A general plot employing Eq. (20) is illustrated in Fig. 13. The first noticeable character is the threshold at which free (and freezable) water appears, also representing the critical amount of

Table 1
Critical water contents, water fusion enthalpy (ΔH) based on one additional gram of sorbed water above the critical contents, partition coefficient (K) between bound and free water, and number of water states for the work presented here and in the literature.

Polymer matrix	Critical water[a] (g/g)	ΔH[a] (J/g)	K[b]	# Water states	Source
PVA[c]	0.675 ± 0.066	339.9 ± 20.5	≈0	3	This work
PVA–FS[d] (10%)	0.565 ± 0.117	308.8 ± 37.3	0.08	3	This work
PVA–FS (20%)	0.459 ± 0.174	297.3 ± 59.9	0.13	3	This work
PVA–FS (30%)	0.352 ± 0.085	235.1 ± 51.9	0.42	3	This work
PVA	0.387	–[e]	0.055	3	Zhang et al. [2]
PVA in aqueous salt solutions	0.385–0.590	–[e]	0.0074–0.160	3	Zhang et al. [2]
PDMS[f]	0.000208 ± 0.000105	333.8 ± 8.9	≈0	2	Lue and Yang [12]
Polyhydroxystyrene	0.083	330	≈0	3	Nakamura et al. [21]
Nafion	0.0785 ± 0.0128	189.7 ± 24.0	0.755	2	Lue and Shieh [30]
PVA hydrogel	0.26–0.40	234–327	–[e]	3	Nagura et al. [5]
Cellulose acetate	0.12–0.13	–[e]	Varied from 0 to 0.081 as water content increases from 0.1 to 0.58.	4	Taniguchi and Horigome [1]
CS[g]	0.401	304.3	0.094	3	Guan et al. [28]
CS/polyether IPN	0.201	272.8	0.221	3	Guan et al. [28]
CS/gelatin	0.361	306.0	0.088	3	Guan et al. [28]
CS/pectin	0.436	201.4	0.654	3	Guan et al. [28]
CS	0.244	289.1	0.055	3	Qu et al. [29]
CS/LA[h] (1:2–2:1)	0.601–0.546	144.4–178.0	1.112–0.713	3	Qu et al. [29]
CS/GA[i]/LA (1:1:1)	0.424	192.3	0.586	3	Qu et al. [29]
CS/GA (1:2–2:1)	0.333–0.377	201.0–231.7	0.517–0.316	3	Qu et al. [29]

[a] Mean ± 95% confidence interval.
[b] Calculated from literature data.
[c] Polyvinyl alcohol.
[d] Fumed silica.
[e] Not available.
[f] Polydimethylsiloxane.
[g] Crosslinked chitosan.
[h] Lactic acid.
[i] Glycolic acid.

non-freezable bound water. From Eq. (10), this threshold is known to be dependant on the critical value of the polymer to form a bound state (λ_c), the filler mass fraction (ϕ), and the hindrance coefficient (ξ). This threshold is proportional to λ_c. At a predetermined λ_c, an increase in diluting filler content (ϕ) or hindrance coefficient (ξ) results in a reduction of this threshold, as shown in the line AB′ in the upper graph of Fig. 13. Under some circumstances, particularly when dissolved solutes produce strong hydration (hygroscopic) effects with water, a negative hindrance coefficient (ξ) is observed. This means the solutes actually bond more water molecules than the pristine polymer films. Salts (e.g., CsCl, LiCl, and LiI), urea, and thiourea have been found to enhance the maximum non-freezable water content [2]. This is illustrated in the line AB″ in the upper graph of Fig. 13.

The second noticeable character is the slope, indicating a change of bound and free (and freezable) water contents with respect to total water content. At low sorption levels, where $\lambda < \lambda_c$, all water in the membrane exists in a bound state. The relationship $Y = X$ holds true in the W_b versus W_t coordinate, as shown in line AB in the lower graph of Fig. 13. Line AB has a slope of unity for plots with X and Y axes in units of grams per grams of dry membrane. At high sorption levels, where $\lambda \geq \lambda_c$, free (and freezable) water starts to appear and the increasing slope depends on K. For $K = 0$, as shown in the case of PVA membrane, additional sorbed water is in a free and freezable state. Therefore a slope of unity is obtained (line DE) in the W_f versus W_t coordinate, with an X intercept at the maximum bound water content [$18\lambda_c(1-\phi)\,(1-\xi\phi/(1-\phi)/44$) from Eq. (10)]. The bound water content does not change with water uptake and the slope is zero in this high sorption range as shown in line BC (Fig. 13, lower graph).

For $K > 0$, as for PVA–FS composites, the relationship between W_b and W_t is similar at low sorption levels ($\lambda < \lambda_c$). However, with water content above the critical bound water content, W_b versus W_t exhibits an increase in the slope, which equals $K/(1+K)$ as shown in line BC′ in Fig. 13 (lower graph). Also, the slope of W_f versus W_t decreases to $1/(1+K)$, as shown in line DE′ (Fig. 13, lower graph). As K increases, the slopes of both W_b and W_f deviate more from zero (the horizontal solid line) and unity (the original DE line) in the high sorption regime. This plot offers a fast and simple analysis tool to illustrate the effect of high water-binding materials on the overall water states sorbed into the membranes.

Notably, the model presented here is not only valid for polymer–filler composite matrix, but is also applicable to homogeneous, heterogeneous or micro-phase separated polymer systems. For instance, many organic solvents in polydimethylsiloxane [12], as well as water in polyhydroxystyrene and in polyvinylpyrrolidone [21,27] exhibit a constant maximum non-freezable solvent content. Their partitioning into freezable and non-freezable states is typical to the BC curve as shown in Fig. 13. On the other hand, water in cellulose acetate [1] chitosan (CS)-based hydrogels [28,29] perfluorosulfonic acid membrane [30], and hydrofluorocarbon polymer electrolyte [31] has been shown to exhibit similar characteristic water state trends, as illustrated in the BC′ curve (Fig. 13). Critical non-freezable bound water contents and partition coefficient (K) results from this study are summarized in Table 1, including calculated values using the above-mentioned literature data. These characteristic parameters can be used to demonstrate the distribution of water into freezable and bound states in various polymer matrices.

The lower graph in Fig. 13 also provides the estimations of water state changes in polymer hybrids with inorganic fillers. For example, Dae et al. [32] reported that silica embedded in a membrane forms a material that can reduce the amount of free water. This result can be fully predicted using Fig. 13. As K increases, free and freezable water content decrease (lower slope) and non-freezable water content increases (higher slope). Therefore, the fraction of free water is reduced. The model developed in this study will enable a better understanding of the distribution of water states into bound water and free (and freezable) water for heterogeneous or hybrid membrane systems. This information will provide insight into film properties, such as water sorption, plasticization, proton conductivity, and methanol permeability. These last two properties are of crucial importance and are believed to impact the performance of polymer electrolytes in fuel cell applications.

5. Conclusion

In this study, the water states in PVA and its nano-composites were characterized using low temperature differential scanning calorimetry. For low water contents, sorbed water was in a bound state. As the water content was increased, free and freezable bound water were formed. The endothermic peak temperature of freezable bound water approached that of free water, becoming indistinguishable from it. Free and freezable bound water contents were combined in one measure. The distribution of free (and freezable) and bound water was determined for PVA composites containing 10–30% FS. Incorporated FS retained more non-freezable bound water and suppressed free (and freezable) water sorption. A mathematical model is proposed to account for water state content as a function of FS concentration. This model takes into consideration the inert filler dilution effect, the equilibrium of bound water to free and freezable water states associated with FS particles, and the suppressed hydrogen-bonding ability of hydroxyl groups in polymer chains caused by the FS shielding. This model can also explain results from other homogeneous or heterogeneous polymeric membrane systems. The corresponding characteristic parameters are summarized in Table 1. Predicted results for this model were in excellent agreement with experimental data.

Acknowledgment

We thank Chang Gung University (BMRP 326) for financial support.

References

[1] Taniguchi Y, Horigome S. J Appl Polym Sci 1975;19(10):2743–8.
[2] Zhang WZ, Satoh M, Komiyama J. J Membr Sci 1989;42(3):303–14.
[3] Fushimi H, Ando I, Iijima T. Polymer 1991;32(2):241–8.
[4] Nagura M, Saitoh H, Gotoh Y, Ohkoshi Y. Polymer 1996;37(25):5649–52.
[5] Nagura M, Takagi N, Katakami H, Gotoh Y, Ohkoshi Y, Koyano T, et al. Polym Gels Network 1997;5(5):455–68.
[6] Wan LS, Huang XJ, Xu ZK. J Phys Chem B 2007;111(5):922–8.
[7] Hietala S, Holmberg S, Näsman J, Ostrovskii D, Paronen M, Serimaa R, et al. Angew Makromol Chem 1997;253:151–67.
[8] Haynes LC, Locke JP. J Microwave Power Electromagn Energy 1995;30(2):124–31.
[9] Liu WG, Yao KD. Polymer 2001;42(8):3943–7.
[10] Gref R, Nguyen QT, Rault J, Neel J. Eur Polym J 1992;28(8):1007–14.
[11] Giménez V, Mantecón A, Cádiz V. Acta Polym 1998;49(9):502–9.
[12] Lue SJ, Yang SW. J Macromol Sci Part B Phys 2005;44(5):711–25.
[13] Edsall JT, Mckenzie HA. Adv Biophys 1983;16:53–183.
[14] Yamane T, Ichiryu T, Nagata M, Ueno A, Shimizu S. Biotechnol Bioeng 1990;36(10):1063–9.
[15] Hoffman AS, Afrassiabi A, Dong LC. J Controlled Release 1986;4(3):213–22.
[16] Okhamafe AO, York P. J Pharm Pharmacol 1985;37(6):385–90.
[17] Taddei P, Balducci F, Simoni R, Monti P. J Mol Struct 2005;744–747:507–14.
[18] Kim DS, Park HB, Rhim JW, Lee YM. Solid State Ionics 2005;176(1–2):117–26.
[19] Chen WF, Kuo PL. Macromolecules 2007;40(6):1987–94.
[20] Lue SJ, Chen JY, Yang JM. J Macromol Sci Part B Phys 2008;47(1):39–51.
[21] Nakamura K, Hatakeyama T, Hatakeyama H. Polymer 1983;24(7):871–6.
[22] Li W, Xue F, Cheng R. Polymer 2005;46(25):12026–31.
[23] Kusumocahyo SP, Sano K, Sudoh M, Kensaka M. Sep Purif Technol 2000;18(2):141–50.
[24] Ito K, Ujihira Y, Higa M. Mater Sci Forum 1997;255–257:305–7.
[25] Puffr R, Sebenda J. J Polym Sci Part C Polym Symp 1967;16:79–93.
[26] Lue SJ, Lee DT, Chen JY, Hu CC, Jean YC, Lai JY. J Membr Sci 2008;325(2):831–9.
[27] Danjo K, Nishio F, Zhow BD, Otsuka A. Chem Pharm Bull 1995;43(11):1958–60.
[28] Guan YL, Shao L, Yao KD. J Appl Polym Sci 1996;61(13):2325–35.
[29] Qu X, Wirsén A, Albertsson AC. Polymer 2000;41(12):4589–98.
[30] Lue SJ, Shieh SJ. J Macromol Sci Part B Phys, doi: 10.1080/00222340802561649.
[31] Siu A, Schmeisser J, Holdcroft S. J Phys Chem B 2006;110(12):6072–80.
[32] Dae SK, Kwang HS, Ho BP, Young ML. Macromol Res 2004;12(4):413–21.